Processing and Application of Ceramics 12 [2] (2018) 111–117
https://doi.org/10.2298/PAC1802111Z



# Dilatrometric sintering study and characterization of alumina-nickel composites

Justyna Zygmuntowicz[1,*], Milena Piątek[2], Aleksandra Miazga[1], Katarzyna Konopka[1], Waldemar Kaszuwara[1]

[1]*Faculty of Materials Science and Engineering, Warsaw University of Technology, 141 Woloska St, 02-507 Warsaw, Poland*
[2]*Institute of Ceramics and Building Materials, Department of Nanotechnology, 9 Postepu St, 02-676 Warsaw, Poland*

Received 25 October 2017; Received in revised form 22 February 2018; Accepted 19 April 2018

## Abstract

*Alumina-nickel composite samples (with 0, 10 and 20 vol.% of Ni) are prepared via slip casting method. Nickel and aluminium oxide powders were used as precursors and diammonium hydrocitrate and citric acid were used as dispersants. The obtained materials were analysed by dilatometry, X-ray diffraction and SEM. The densities were measured by Archimedes method and the hardness and fracture toughness were determined by using Vickers hardness tester. Special attention was paid to the linear shrinkage and the effective coefficient of thermal expansion measurements. The shrinkage curves were obtained by dilatometry test in a heating mode. It was shown that the increased amount of Ni particles in $Al_2O_3$-Ni composite structure causes reduction of starting densification temperature, increasing temperature of maximum densification and decreasing total shrinkage of the sample during sintering.*

***Keywords:*** *$Al_2O_3$/Ni composites, slip casting, structural characterization, mechanical properties*

## I. Introduction

The processing and properties of ceramic-metal composites have been areas of considerable interest over the past few decades [1,2]. Significant attention has been paid to the composites of the alumina-nickel system due to their interesting properties [3,4]. In addition to increased fracture toughness, the composites of this system are characterized by high hardness, low abrasive wear, the ability to work at high temperatures and good corrosion resistance. The improvement of mechanical properties of alumina ceramics via its reinforcement with nickel particles is achieved due to number of factors. The first is the interaction of the cracks with the metallic phase particles through mechanisms such as crack deflection, microcrack toughening, crack blunting or crack bridging. The second is toughening by residual stress due to mismatch between the coefficients of thermal expansion of the ceramic matrix and reinforcing phase [5]. The presence of nickel in alumina matrix results in accumulation of compressive stress, which can increase crack resistance of the material.

Alumina-nickel composites are currently being formed through different processes, like classical powder metallurgy or spark plasma sintering [6–8]. Particular attention is paid to colloidal methods such a slip casting [9] or gel-casting [10]. The great advantage of these methods is the ability to form details of complex shapes, without costly finishing with the use of diamond tools. Moreover, by controlling the properties of the used slurries one can verify the obtained microstructure of the ceramic-metal composites [11]. Through the adjustable particles stabilization in suspension we can achieve a high level of dispersion of metallic phase in ceramic matrix, which preferably affects the strength of the material. Further, composite materials formed by colloidal methods are characterized by high microstructural uniformity and reliability [12].

During the manufacturing process of composite materials, the sintering process plays a key role. Manufacturing of near-net-complex shape components requires processing control at each stage, especially during sin-

*Corresponding author: tel: + 48 22 2348138,
e-mail: *justyna.zygmuntowicz@inmat.pw.edu.pl*

tering. In order to obtain a high-quality element with predicted properties it is necessary to know the processes taking place during the sintering – control of shrinkage of the material. Several studies have been devoted to the sintering study of alumina based materials. In literature, there are studies on the degradation of organic additives such as deflocculants or binders present in the green body samples after shaping process [13,14]. Dilatometric studies of alumina [15,16] and alumina based composites were also made [17–20], but a deep characterization of the alumina-metal composites is much less frequent. The dilatometric study of ceramic-metal composites is a complicated issue. Therefore, they are the subject of continuous research.

Furthermore, the addition of the metallic phase significantly affects the thermal expansion coefficient of the material. This is an important parameter, especially for high temperature applications.

In the present work, alumina-nickel composites were formed by slip casting method and conventional pressureless sintering. The aim of this work is to investigate the effect of nickel addition on sintering of $Al_2O_3$-Ni composite. The analysis of the sintering process of the composites will allow to fully plan the technological process of material production. This is particularly important for complex shapes that can be obtained by slip casting method. Despite many studies on $Al_2O_3$-Ni composites [2–10], there is no such research in the literature up to now.

## II. Experimental

The presented experiments were carried out with $\alpha$-$Al_2O_3$ (TM-DAR, Taimei Chemicals, Japan) and nickel powder (Sigma-Aldrich). The purity of both powders was 99.99%. The densities of the powders were determined by a helium pycnometer, AccuPyc 1340 II. The dispersants used in the ceramic slurries were diammonium hydrocitrate, DAC (puriss, POCh, Poland) and citric acid, CA (≥ 99.5% Sigma-Aldrich).

Three types of $Al_2O_3$-Ni composite samples, with 0, 10 and 20 vol.% of Ni, were prepared. The composite samples were obtained according to the slip casting method schematically shown in Fig. 1. The mixture of the slip casting components was prepared in several steps. First, the components of the ceramic slurry were dissolved in distilled water. The dispersants as a mixture of diammonium hydrocitrate (0.30 wt.% in the case of starting powders) and citric acid (0.10 wt.% in case of both powders) were used. Alumina and nickel powders were then added and the slurry was ball-milled for 1.5 h for good homogenization. In the next stage the slurries were degassed in a device for automatic slurry mixing and degassing (ARE-250 produced by Thinky Corporation) for 3 min at the rate of 1500 rpm. The mixture was then cast into identical gypsum moulds and the obtained specimens were dried for 24 h at 40 °C. The dried and shrunk sample could be removed from the gypsum mould easily. The sample was sintered at 1400 °C for 2 h in an atmosphere of helium. During the sintering, the heating and cooling rate were 2 °C/min.

The linear shrinkage and the effective coefficient of thermal expansion measurements were determined by dilatometer DIL 402 E (Netzsch, Germany). The composite samples were shaped into cylindrical rod of 10–14 mm in length with 6–8 mm diameter, the transversal external surfaces being polished to guarantee plan-parallel surfaces for precise positioning within the measuring head. The samples were subjected to the constant heating rate of 10 °C/min up to 1400 °C/10 min, in flowing helium and in a furnace with graphite heating elements. Green samples were used in shrinkage measurements while the effective coefficient of thermal expansion measurements was performed using samples after sintering at 1400 °C. Recording the thermal expansion ensures the determination of the coefficient of thermal linear expansion in temperature range from 30 °C to 1400 °C and from 1400 °C to 50 °C. Within the investigated temperature range, the instrumental error was corrected using a reference graphite sample. Calibration measurements were carried out under the same conditions (in terms of the course of the temperature curve, atmosphere, gas flow rate) as the proper measurements to determine the signals related to the expansion of the device components and to correct the results obtained during the proper measurement. The determination of the change in linear dimension during shrinkage makes it possible to establish the necessary technical parameters like the commencement and termination of the sintering of the ceramic and composites bodies which afford an indirect assessment of the sintering kinetics.

X-ray diffraction (XRD) measurements were performed by Rigaku MiniFlex II X-ray diffractometer with Cu $K_\alpha$ ($\lambda$ = 1.54178 Å) incident radiation. The diffraction patterns were collected at room temperature in the $2\theta$ range from 20° to 100°, with step of 0.02° and counting time of 0.5 s.

The densities of the samples were measured by the Archimedes method in distilled water and twenty sam-

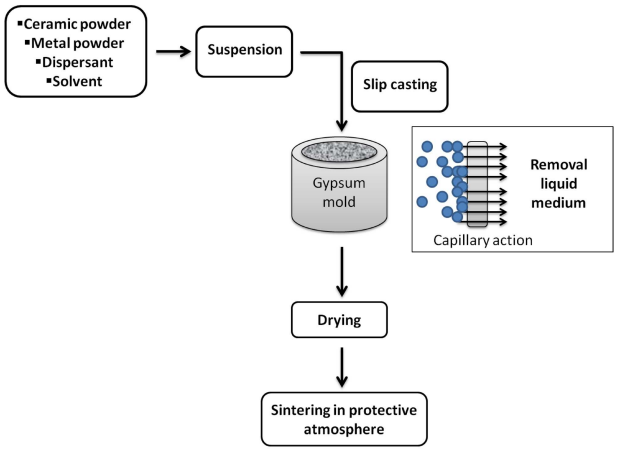


**Figure 1. Scheme for the preparation of composites by slip casting**

ples in each series were used. The observation of cross-section and fracture of the composite samples was performed using scanning electron microscope (SEM HITACHI SU-70, Japan). The cross-sections were prepared by cutting the samples along the axial direction with diamond saw. The polished cross sections were prepared by grinding and polishing with 1 μm diamond paste.

Vickers hardness was measured with a Vickers hardness tester (HVS-30T, Huatec Group Corporation) with the use of the indentation method under the load of 98 N and holding time of 10 s. All tests were done for ten samples. The $K_{IC}$ values were determined using the direct crack measurement method. Based on the measurements of the crack length propagated from the corner of the hardness indentation, the fracture toughness of the material ($K_{IC}$) was determined. In this experiment, a Vickers hardness indenter was adjusted to propagate until what is called median crack on the surface. The $K_{IC}$ values in this case were calculated using the following formula [21]:

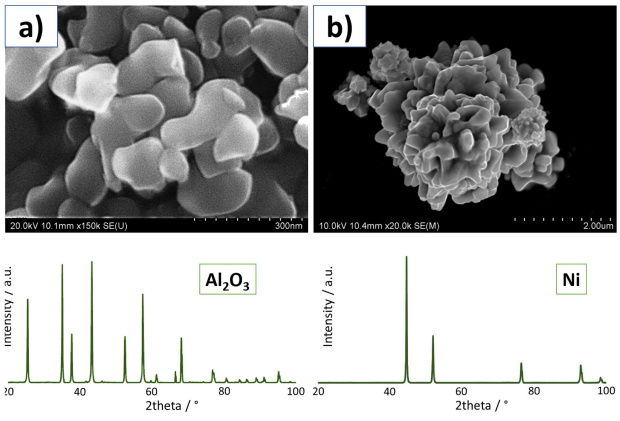


**Figure 2. Morphology and X-ray diffraction (XRD) patterns of the starting powders: a) $Al_2O_3$ and b) Ni**

$$K_{IC} = 0.067\left(\frac{E}{H_V}\right)^{0.4} \cdot \left(\frac{c}{a}\right)^{-1.5} \cdot H_V \cdot \sqrt{a} \qquad (1)$$

where $H_V$ is Vickers hardness, $E$ is Young's modulus, $a$ is one half of the indent diagonal length, $c$ is crack length.

## III. Results and discussion

The precursor alumina powder has average particle size $D_{50}$ = 150 nm, specific surface area of 12.50 $m^2/g$, and density of 3.96 $g/cm^3$. The nickel powder has the average particle size $D_{50}$ = 4.5 μm, specific surface area of 0.45 $m^2/g$, and density 8.90 $g/cm^3$. Figure 2 shows the morphology of the starting powders. The SEM observations revealed that the $\alpha$-$Al_2O_3$ powder is highly agglomerated. The XRD study showed that powders are single-phase: corundum for alumina powder (JCPDS-PDF #046-1212) and cubic nickel phase (JCPDS-PDF #004-0850).

Linear shrinkages and linear shrinkage rates for the green samples after dilatometric experiments are shown in Fig. 3. Linear shrinkage rates facilitate the investigation of the sintering kinetics involved in the densification process of aluminium oxide. The sintering behaviour is clearly related to the additive composition investigated. Total shrinkage of samples, temperature of densification start and temperature of maximum densification for individual samples are summarized in Table 1.

Dilatometric tests showed that the addition of Ni particles into $Al_2O_3$ matrix shifted starting densification temperature for ~8 °C in the case of the composite with 10 vol.% of Ni and ~30 °C when 20 vol.% of Ni was added, in comparison to the pure $Al_2O_3$ sample. The maximum densification rate for the pure $Al_2O_3$ sample is at about 1258 °C, whereas this temperature is increased to 1277 °C and 1279 °C for the composites with

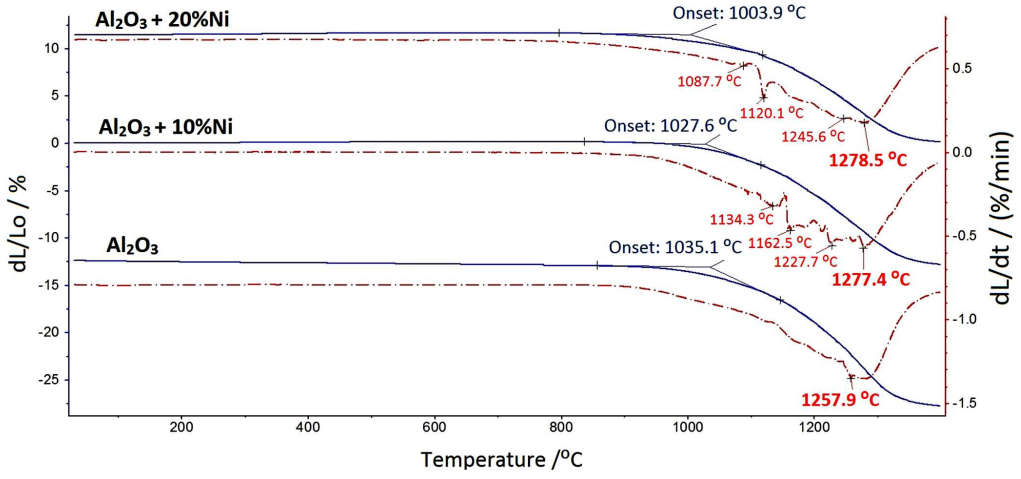


**Figure 3. Linear shrinkage and linear shrinkage rate curves of $Al_2O_3$, $Al_2O_3$-10 vol.% Ni and $Al_2O_3$-20 vol.% Ni green samples as a function of temperature**

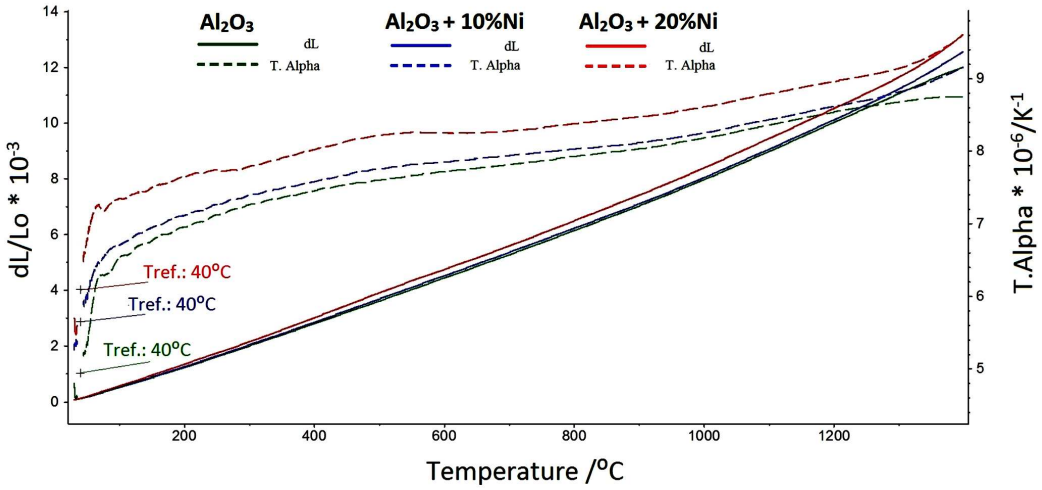


**Figure 4. Thermal expansion coefficient of $Al_2O_3$ matrix and $Al_2O_3$-Ni composites as a function of temperature**

**Table 1. Total shrinkage of samples, starting densification temperature and temperature of maximal densification for individual samples**

| Sample | $T_{sd}$ [°C] | $T_{md}$ [°C] | Shrinkage [%] |
|---|---|---|---|
| $Al_2O_3$ | 1035 | 1258 | 14.12 |
| $Al_2O_3$ – 10 vol.% Ni | 1027 | 1277 | 12.79 |
| $Al_2O_3$ – 20 vol.% Ni | 1003 | 1279 | 11.28 |

*$T_{sd}$ - Starting densification temperature*

*$T_{md}$ - Temperature of maximal densification*

10 and 20 vol.% of Ni, respectively. The total shrinkage of the $Al_2O_3$ sample reached ~14% at 1400 °C. Dilatometric experiments confirmed that 10 vol.% and 20 vol.% nickel particles addition leads to the decrease of the total shrinkage at 1400 °C to 12.79% and 11.28%, respectively. Thus, the addition of nickel particles in alumina matrix, causes decrease of the starting densification temperature, increase of the temperature where the maximum densification rate occurs, and the decrease of the total shrinkage. Base on literature data, it was found that these results are caused by the fact that during sintering, the nickel particles are in a liquid phase [22] and addition of nickel particles hinder the sintering process [3,23].

For the alumina and nickel particles dispersed in the ceramic matrix, a great mismatch occurs between their thermal expansion coefficients. The addition of particles characterized by a higher thermal expansion coefficient than the matrix causes compression of the matrix in the region nearby the particle. The increase of the amount of nickel increases the forces resulting from the mismatch of thermal expansion and as the consequence leads to the decrease of the total shrinkage. Measurement of thermal expansion coefficient is used to determine the rate at which a material expands as a function of temperature. The thermal expansion characteristics of the $Al_2O_3$ matrix and $Al_2O_3$-Ni composites are shown in Fig. 4 and Table 2.

According to the literature data, the presence of four peaks in the curve of shrinkage rate in case of $Al_2O_3$-Ni composites with 10 and 20 vol.% of Ni is an indirect evidence of the availability of hard agglomerates, which could result in a lower sintering efficiency. The thermal expansion coefficient of $Al_2O_3$-Ni samples increases with an increasing amount of Ni in their structure. For all samples values of thermal expansion coefficients were increased within whole measurement range, i.e. up to 1400 °C. For example, linear thermal expansion coefficient of $Al_2O_3$-Ni composite with 20 vol.% of Ni increases from $7.35\times10^{-6}$ K$^{-1}$ at 100 °C to $9.14\times10^{-6}$ K$^{-1}$ at 1300 °C.

X-ray diffraction patterns recorded from the sintered ceramic and composite samples are shown in Fig. 5. As it can be seen, the observed peaks indicated the presence of alumina and nickel phases and no other phases were detected. The use of protective atmosphere (helium) prevents the oxidation of nickel during sintering so that we have obtained a two-phase structure of the composite samples. The peaks are not widened which proves the high crystallinity of the samples. The two-phase structure of the composite is the most advanta-

**Table 2. Coefficients of linear thermal expansion of $Al_2O_3$ matrix and $Al_2O_3$-Ni composites**

| Sample | Coefficient of linear thermal expansion, $\alpha$ [$10^{-6}$ K$^{-1}$] | | | | |
|---|---|---|---|---|---|
| | 40–100 °C | 40–300 °C | 40-500 °C | 40–1000 °C | 40–1300 °C |
| $Al_2O_3$ | 6.54 | 7.26 | 7.61 | 8.18 | 8.68 |
| $Al_2O_3$ – 10 vol.% Ni | 6.71 | 7.40 | 7.76 | 8.26 | 8.81 |
| $Al_2O_3$ – 20 vol.% Ni | 7.35 | 7.79 | 8.21 | 8.61 | 9.14 |

**Table 3. Selected properties of $Al_2O_3$ and $Al_2O_3$-Ni samples**

| Property | $Al_2O_3$ | $Al_2O_3$ – 10 vol.% Ni | $Al_2O_3$ – 20 vol.% Ni |
|---|---|---|---|
| Theoretical density [g/cm$^3$] | 3.96 | 4.45 | 4.95 |
| Relative density [%TD] | 98.21 ± 0.52 | 97.68 ± 0.70 | 96.20 ± 0.35 |
| Soaking [%] | 0.08 ± 0.02 | 0.13 ± 0.03 | 0.20 ± 0.05 |
| Open porosity [%] | 0.78 ± 0.32 | 0.68 ±0.22 | 0.92 ± 0.38 |
| Hardness [GPa] | 16.65 ± 0.53 | 11.35 ± 0.78 | 9.07 ± 0.62 |
| Fracture toughness [MPa·m$^{0.5}$] | 4.10 ± 0.27 | 8.29 ± 0.33 | 10.78 ± 0.49 |

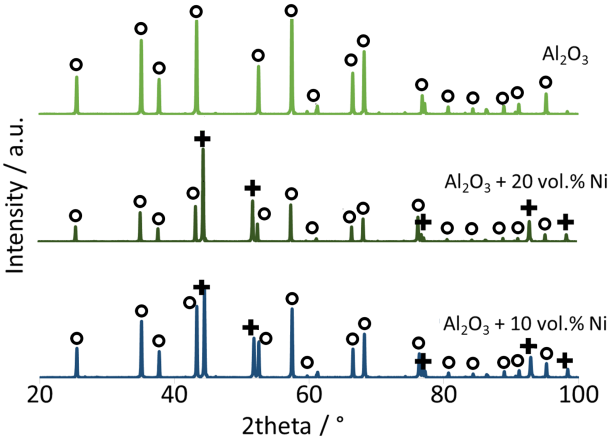


**Figure 5. XRD patterns of monolithic $Al_2O_3$ and $Al_2O_3$-Ni composites (o - $\alpha$-$Al_2O_3$, + - Ni)**

geous from the point of view of its mechanical properties.

The selected properties of the materials are presented in Table 3. It was found that in the case of $Al_2O_3$-Ni composites the relative density is a slightly lower than in the case of the pure $Al_2O_3$ sample. The measurement showed that the relative density of the sintered samples decreases from 98 %TD to 96 %TD when the amount of nickel particles is increased from 0 to 20 vol.%. The decrease in density of composites is associated with the increased number of agglomerated metallic particles.

Micrographs in Fig. 6 show cross sections and fracture surfaces of unreinforced $Al_2O_3$ and $Al_2O_3$-Ni composites. The bright areas are nickel particles. Based on the presented micrographs, it can be concluded that the applied method enables an uniformly distributed metallic particles in composite matrix. Few nickel agglomerates are visible. The observations of fracture showed that the nickel particles are well-bonded to ceramic matrix. It can be observed that the sintering process allowed to obtained samples almost free of pores, as confirmed by measurements of density (Table 3). Furthermore, the SEM analyses of fracture clearly indicate a lack of interlayer between alumina and nickel. It can be due to the coagulation of alumina into bigger particles (Ni) or diffusion of nickel into alumina matrix or the other way around. Aluminium oxide cracked mainly intergranulary. Based on the observations of fractures, no impact of nickel addition on alumina grain size was found.

In addition, the influence of nickel addition on the mechanical properties of the fabricated materials was investigated. The polished samples were used for Vickers hardness measurements. The hardness of the pure $Al_2O_3$ samples is 16.65±0.53 GPa. For the samples containing 10 and 20 vol.% of Ni the hardness value was 11.35 ± 0.78 and 9.07 ± 0.62 GPa, respectively. The obtained hardness results correspond to the change in the distribution of Ni in the samples. It was observed that the composite with 20 vol.% of Ni is characterized by

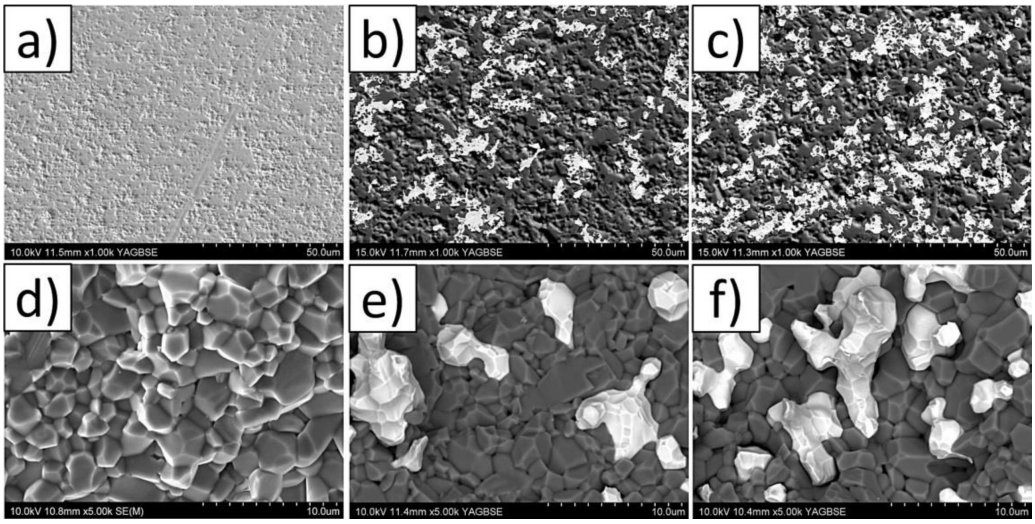


**Figure 6. SEM images of the samples: a,d) $Al_2O_3$, b,e) $Al_2O_3$-10 vol.% Ni, c,f) $Al_2O_3$-20 vol.% Ni (cross sections and fractured surfaces)**

the lower hardness. From the above results, it may be concluded that *inter alia* the plasticity of the Ni particles influences the hardness.

One of the most important parameters for ceramic matrix composites is fracture toughness. It was observed that all samples with nickel modified matrix showed significant improvement in the fracture toughness compared to the pure alumina samples. Based on the measurements of the crack length propagated from the corner of the hardness indentation, the fracture toughness of the pure $Al_2O_3$ was equal to 4.10 ± 0.27 MPa·m$^{0.5}$. In the case of the $Al_2O_3$-Ni composites with 10 and 20 vol.% of Ni the fracture toughness was 8.29 ± 0.33 MPa·m$^{0.5}$ and 10.78 ± 0.49 MPa·m$^{0.5}$, respectively. The addition of the metallic phase increases the fracture toughness. Thus, the composites containing 20 vol.% of nickel achieves 2.5 times higher fracture toughness than the pure $Al_2O_3$. The increase of the fracture toughness in composites was due to the several factors. Crack bridging and branching [24], delamination [25] and the singly and doubly deflected crack [4,5,25] were responsible for fracture toughness improvement in the ceramic matrix composites. The result obtained for the fracture toughness provided evidence of influence of the metal particles distribution on mechanical properties of composites.

## IV. Conclusions

Slip casting method was used to obtain $Al_2O_3$-Ni composites, which are characterized by an uniformly distributed metal particles throughout the volume of the alumina matrix. The XRD confirmed that the sintered composites consist of $\alpha$-$Al_2O_3$ and Ni without secondary phases. Dilatometric experiments revealed the presence of several shrinkage peaks during sintering of $Al_2O_3$ matrix and $Al_2O_3$-Ni composites. This is an indirect evidence for the presence of the hard agglomerates in precursor powders. Increasing amount of Ni in $Al_2O_3$-Ni structure decreases the temperature of densification start, increases temperature of maximum densification and also decreases total shrinkage of the samples during sintering. Nickel addition has also influence on thermal expansion coefficient and mechanical properties. The thermal expansion coefficient of $Al_2O_3$-Ni samples and fracture toughness increases, whereas the hardness decreases with an increasing amount of Ni.

**Acknowledgements:** The results presented in this paper were obtained within the project (PRELUDIUM 12) from the National Science Centre of Poland (NCN), Agreement No. 2016/23/N/ST8/00234.

## References

1. M. Rosso, "Ceramic and metal matrix composites: Routes and properties", *J. Mater. Process. Technol.*, **175** [1-3] (2006) 364–375.
2. T. Rodriguez-Suarez, J.F. Bartolome, J.S. Moya, "Mechanical and tribological properties of ceramic/metal composites: A review of phenomena spanning from the nanometer to the micrometer length scale", *J. Eur. Ceram. Soc.*, **32** [15] (2012) 3887–3898.
3. W.H. Tuan, R.J. Brook, "The toughening of alumina with nickel inclusions", *J. Eur. Ceram. Soc.*, **6** [1] (1990) 31–37.
4. W.G. Fahrenholtz, D.T. Ellerby, R.E. Loehman, "$Al_2O_3$-Ni composites with high strength and fracture toughness", *J. Am. Ceram. Soc.*, **83** [5] (2000) 1279–1280.
5. X. Sun, J.A. Yeomans, "Microstructure and fracture toughness of nickel particle toughened alumina matrix composites", *J. Mater. Sci.*, **31** [4] (1996) 875–880.
6. R.T. Chen, W.H. Tuan, "Pressureless sintering of $Al_2O_3$/Ni nanocomposites", *J. Eur. Ceram. Soc.*, **19** [4] (1999) 463–468.
7. T. Sekino, T. Nakajuma, S. Ueda, K. Niihara, "Reduction and sintering of a nickel-dispersed-alumina composite and its properties", *J. Am. Ceram. Soc.*, **80** [5] (1997) 1139–1148.
8. J. Zygmuntowicz, A. Miazga, K. Konopka, K. Jędrysiak, W. Kaszuwara, "Alumina matrix ceramic-nickel composites formed by centrifugal slip casting", *Process. Appl. Ceram.*, **9** [4] (2015) 199–202.
9. A. Javier Sánchez-Herencia, N. Hernández, R. Moreno, "Rheological behavior and slip casting of $Al_2O_3$-Ni aqueous suspensions", *J. Am. Ceram. Soc.*, **89** [6] (2006) 1890–1896.
10. A. Miazga, K. Konopka, M. Gizowska, M. Szafran, "Preparation of $Al_2O_3$-Ni cermet composites by aqueous gelcasting", *Powder Metall. Met. Ceram.*, **52** [9-10] (2014) 567–571.
11. M. Gizowska, K. Konopka, M. Szafran, "Properties of water-based slurries for fabrication of ceramic-metal composites by slip casting method", *Arch. Metall. Mater.*, **56** [4] (2011) 1105–1110.
12. R. Moreno, "Colloidal processing of ceramic-ceramic and ceramic-metal composites", *Ceram. Trans.*, **225** (2011) 147–159.
13. P. Wiecinska, "Thermal degradation of organic additives used in colloidal shaping of ceramics investigated by the coupled DTA/TG/MS analysis", *J. Therm. Anal. Calorim.*, **123** [2] (2016) 1419–1430.
14. J. Zygmuntowicz, P. Wiecińska, A. Miazga, K. Konopka, W. Kaszuwara, "$Al_2O_3$/Ni functionally graded materials (FGM) obtained by centrifugal-slip casting method", *J. Therm. Anal. Calorim.*, **130** [1] (2017) 123–130.
15. P. Palmero, M. Lombardi, "Sintering of a nano-crystalline metastable alumina", *J. Therm. Anal. Calorim.*, **97** [1] (2009) 191–196.
16. Z. Holkova, L. Pach, V. Kovar, Š. Svetik, "Kinetic study of $Al_2O_3$ sintering by dilatometry", *Ceramics - Silikáty*, **47** [1] (2003) 13–19.
17. O.R.K. Montedo, P.C. Milak, F.D. Minatto, R.B. Nuernberg, C.A. Faller, A.P.N. Oliveira, A. De Noni, "Effect of a LZSA glass-ceramic addition on the sintering behavior of alumina", *J. Therm. Anal. Calorim.*, **124** [124] (2016) 241–249.
18. K. Maca, V. Pouchly, D. Drdlika, H. Hadraba, Z. Chlup, "Dilatometric study of anisotropic sintering of alumina/zirconia laminates with controlled fracture behaviour", *J. Eur. Ceram. Soc.*, **37** [14] (2017) 4287–4295.
19. A.P. Surzhikov, T.S. Frangulyan, S.A. Ghyngazov, P. Vasiliev, "A dilatometric study of sintering of compos-

ite ceramics manufactured from ultrafine $ZrO_2$(Y)-$Al_2O_3$ powders under different thermal-temporal firing conditions", *Russian Phys. J.*, **57** [3] (2014) 411–415.
20. J.M. Auger, S. Saunier, F. Valdivieso, "Characterisation of sintering of alumina matrix-stainless steel dispersion composite and interaction between chromium, carbon and alumina during powder metallurgy process", *Powder Metal.*, **54** [4] (2011) 522–528.
21. K. Niihara, "A fracture mechanics analysis of indentation", *J. Mater. Sci. Lett.*, **2** (1983) 221–223.
22. M. Gizowska, A. Miazga , K. Konopka, M. Szafran, "The influence of sintering temperature on properties of $Al_2O_3$-Ni composites", *Compos. Theory Pract.*, **12** [1] (2012) 33–38.
23. R.Z. Chen, W.H. Tuan, "Pressureless sintering of $Al_2O_3$/Ni nanocomposites", *J. Eur. Ceram. Soc.*, **19** [4] (1999) 463–468.
24. J. Liu, H. Yan, M.J. Reece, K. Jiang, "Toughening of zirconia/alumina composites by the addition of graphene platelets", *J. Eur. Ceram. Soc.*, **32** [16] (2012) 4185–4193.
25. K. Konopka, A. Miazga, J. Właszczuk, "Fracture toughness of $Al_2O_3$-Ni composites with nickel aluminate spinel phase $NiAl_2O_4$", *Compos. Theory Pract.*, **11** [3] (2011) 197–201.